Astron. Astrophys. 326, 263–270 (1997)

ASTRONOMY
AND
ASTROPHYSICS

A study on solar dust ring formation based on fractal dust models

H. Kimura[1], **H. Ishimoto**[2], **and T. Mukai**[2]

[1] Max-Planck-Institut für Aeronomie, Postfach 20, D-37189, Katlenburg-Lindau, Germany
[2] The Graduate School of Science and Technology, Kobe University, Nada, Kobe 657, Japan

Received 31 July 1996 / Accepted 10 April 1997

Abstract. Using the fractal aggregate model for circumsolar dust grains, the nature of the circumsolar dust clouds is examined. As a fractal dimension of the aggregate decreases, the porosity of the aggregate increases. Consequently, its temperature becomes independent of its size, and approaches that of its constituent particles. This evidence suggests that the fractal aggregates with different sizes and made of the same chemical components sublimate at the same solar distance. This implies that the distance of the sublimation zone depends on the chemical composition alone. We have found that the aggregates consisting of silicate material, as well as carbon material, sublimate in the solar F-corona. On the other hand, a ratio of radiation pressure force to solar gravity on the fractal aggregate scarcely increases with decreasing size due to sublimation, in contrast with a strong dependence of its ratio on its size for a compact sphere.

Our computer simulation for dynamical evolution of fractal aggregates suggests that they produce a narrow ring structure in the circumsolar dust cloud, compared with that expected for spherical dust grains. When the aggregates have more fluffy structure with a small fractal dimension, however, it is found that the circumsolar dust clouds would make no remarkable ring structure.

Key words: interplanetary medium – Sun: corona – infrared: solar system

1. Introduction

On the basis of dynamical evolution for circumsolar dust grains, an accumulation of circumsolar dust grains (the solar dust ring) at their sublimation zone has been proposed by Belton (1966). The circumsolar dust grains seem to be supplied from the zodiacal dust clouds continually because interplanetary dust particles, which are observed as the zodiacal light, gradually spiral toward the sun under the Poynting-Robertson drag force. Even though the circumsolar dust grains consist of refractory materials, they suffer from sublimation because of their high temperature near the sun. Since the temperature of a spherical grain strongly depends on its radius, those grains with different initial radii sublimate at various solar distances from the sun. Under the sublimation, a ratio β of the radiation pressure force to the solar gravitational force on a grain increases with decreasing radius when the radius is larger than 0.5 μm. The increase of the β ratio counterbalances the Poynting-Robertson drag force and thus the sublimating grains are piled up at their sublimation zone. Consequently, a collection of the sublimating grains with different radii creates a solar dust ring having a wide structure around the sun.

The hypothetical dust ring around the sun has been supported by an excessive near-infrared F-coronal brightness at 4 solar radii ($R_\odot$) from the sun, since it was detected in the solar eclipse of 1966 by MacQueen (1968) and Peterson (1967, 1969) independently. Mukai et al. (1974) have indicated that the sharp hump of the near-infrared brightness in the solar F-corona arises from the solar dust ring consisting of carbon (graphite) grains because graphite grains with different initial radii sublimate at a narrower region in the F-corona than that from silicate. On the other hand, the intermediate infrared observations have suggested an existence of silicate materials in the F-corona referring to their high brightness at a wavelength of 10 μm (Léna et al. 1974; Mankin et al. 1974). However, the authors note that the observed brightness may contain atmospheric contributions. Lamy (1974a) has shown from numerical calculations that the sublimating grains consisting of silicate (obsidian) stay in the solar distance ranges from 2.2 to 3.5 $R_\odot$ before they completely disappear due to sublimation. Mukai & Yamamoto (1979) have confirmed that the model of the solar dust rings composed of obsidian and graphite grains explains the F-coronal observations in both the near-infrared and the intermediate infrared. In addition, they have concluded that the spatial number density of spherical grains in the sublimation zone becomes five times larger for silicate and ten times larger for carbon than that expected from their radial velocities under the Poynting-Robertson effect alone.

Send offprint requests to: H. Kimura

In the visible brightness of the solar F-corona, no hump feature has been observed to date (cf. Koutchmy & Lamy 1985). On the contrary, calculated visible brightness based on the model of the solar dust rings shows an enhancement due to an accumulation of small (0.01-0.1 μm) silicate particles (Mukai & Yamamoto 1979). Using the blackbody approximation for dust temperature, Mann (1992) has indicated that a combination of thermal emission and scattered light brightness without the solar dust ring can explain the observed brightness feature in both the visible and the near-infrared wavelength. This result arises from the fact that the thermal emission brightness shows a peak at the edge of the dust-free zone (Peterson 1963), whereas the peak feature is absent in the scattered light brightness. Furthermore, Mann (1992) has pointed out that the accumulation of circumsolar dust grains expected by Mukai & Yamamoto (1979) is too large to explain the smooth curve of visible F-coronal brightness, or that the hypothetical dust ring does not exist.

For the last two decades, many interplanetary dust particles have been collected in the Earth's stratosphere (Brownlee 1976). Photographs of the particles taken by an electron microscope have clarified an existence of irregularly shaped dust particles in the solar system, which have an agglomerate structure of many constituent particles with small radii of $0.01 - 0.1$ μm. Therefore, it is natural to assume that circumsolar dust grains have an irregular shape with a fluffy structure. In previous studies concerning the solar dust clouds, however, it has been assumed that the circumsolar dust grains have a spherical shape with a homogeneous structure for simplicity. Recently, Mukai et al. (1992) have found that β ratios of irregularly shaped porous dust particles become independent of their radii. The porous particles are described as fractal aggregates according to the model explained in Mukai et al. (1992) and is hereafter referred to as the fractal dust model. An increase of β due to sublimation is small for a fractal dust aggregate, and consequently the counterforce to the Poynting-Robertson drag should become weak. Moreover, Kozasa et al. (1992) have shown an independence of the aggregate's temperature consisting of magnetite material on its radius. Such a size-independence of aggregate temperature will reduce the predicted width of the solar dust ring, because the aggregates with different sizes sublime at nearly the same solar distance. It should be noted, however, that the temperature of fractal dust depends strongly on its chemical composition (Mann et al. 1994). Taking into account the size-independence of β and the temperatures of fractal aggregates, it is expected that the solar dust ring of fluffy aggregates will show less accumulation of the dust at a narrower sublimation region than that expected for spherical dust particles with homogeneous structure, or that the dust ring no longer exists. In this paper, therefore, we reexamine the existence of the solar dust ring(s) based on the fractal dust model.

2. Fractal dust model for interplanetary dust particles

As a model of fluffy dust aggregate, we use two extreme cases of fractal aggregates, i.e., BPCA (Ballistic Particle Cluster Aggregate) and BCCA (Ballistic Cluster Cluster Aggregate), consisting of a collection of small spherical particles having the same radii s_0. The structure of the fractal aggregate is characterized by a fractal dimension, which is 2.98 for BPCA and 1.93 for BCCA referring to the results of Mukai et al. (1992). The fractal dimension D is determined by a relation between the number of the constituent particles N and the normalized characteristic radius s/s_0 of the aggregate as

$$N = \alpha\left(\frac{s}{s_0}\right)^D, \tag{1}$$

where s is the characteristic radius of the dust aggregate defined in Kozasa et al. (1992). The factor α depends on the coagulation process.

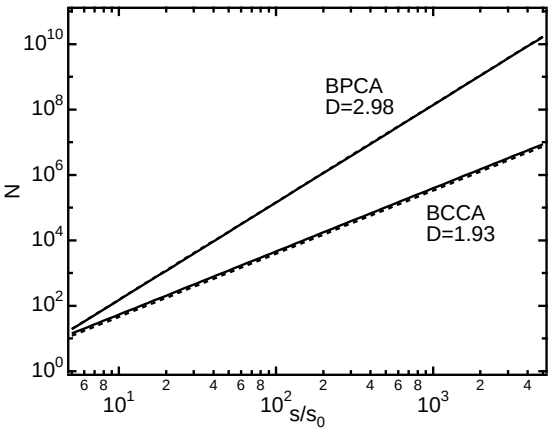

Fig. 1. The relation between the number of the constituent particles, N, and the normalized radius of the aggregate, s/s_0, where s and s_0 denote the characteristic radius of the aggregate and the radius of the constituent particles, respectively. Solid line: $\log\alpha = -0.576D + 0.915$; dashed line: $\log\alpha = -0.5D + 0.7$. For BPCA, both lines are nearly overlapped.

In the following calculations, we adopt a relation of $\log\alpha = -0.576D + 0.915$ for the fitting factor α from Blum & Kozasa (1992). Although the relation between α and D differs from $\log\alpha = -0.5D + 0.7$ used in Mukai et al. (1992), the difference of the α values is negligible as shown in Fig. 1. In contrast to a BCCA, a BPCA with the same radius s has a somewhat compact structure because the number N of the constituent particles for the BPCA exceeds that for the BCCA. A porosity po of the aggregate with the characteristic radius s, which is defined as $po = 1 - \alpha\left(s/s_0\right)^{D-3}$, increases with decreasing fractal dimension, whereas for a compact sphere of homogeneous material, $p = 0$ with $\alpha = 1$ and $D = 3$.

In order to deduce the optical properties of the dust aggregate, it is convenient to use the Bruggeman mixing rule to calculate the effective dielectric function of the aggregate (Jones 1988). Note the applicability of this rule in that the wavelength λ is considerably large compared with the radius s_0 of the constituent particles. The effective dielectric function ϵ_{eff} of the aggregate composed of the n-component materials with

Table 1. Physical parameters of silicate and carbon. The bulk density of a constituent particle, the mean molecular weight, the latent heat per unit mass of sublimated molecules, and the constant number related with the saturated vapor pressure are given by ρ, μ, L, and b, respectively.

	ρ (kg/m^3)	μ	L (J/kg)	b
silicate	2.37×10^3 [a]	67.0 [a]	7.12×10^6 [b]	30.0 [b]
carbon	1.95×10^3 [c]	12.0 [c]	7.27×10^7 [d]	36.0 [d]

[a] Lamy (1974b)
[b] Centolanzi & Chapman (1966)
[c] Lide (1994)
[d] Clarke & Fox (1969)

dielectric function ϵ_i is derived from the equation:

$$\sum_{i=1}^{n} f_i \frac{\epsilon_i - \epsilon_{eff}}{\epsilon_i + 2\epsilon_{eff}} = 0, \tag{2}$$

where $f_i = \tilde{f}_i(1 - po)$ is the volume fraction occupied by the constituent material of type i having its content $\tilde{f}_i$. Silicate and carbon are used as the constituent materials of the composite aggregate to represent the dielectric and absorbing materials, respectively. Furthermore, the vacuum is taken as the constituent material with $f_i = po$ and $\epsilon_i = 1$. Consequently, the optical properties of the fractal aggregate are obtained as a homogeneous sphere with its dielectric function ϵ_{eff} using Mie theory.

The dielectric functions ϵ_i are derived from the complex refractive indices (n, k), using $(n - ik)^2 = \epsilon_i$. The complex refractive indices for silicate and carbon used in this paper are cited from Mukai (1990) and Hanner (1987), respectively. Other physical parameters for silicate and carbon are listed in Table 1. The constant b in Table 1 is defined as the constant b_i in the saturated vapor pressure given in Eq. (6).

3. Equilibrium temperature

The rates of absorbed energy E_a and emitted energy E_r for the fractal aggregate with the effective cross section A are described as

$$E_a = \Omega \int_0^\infty A Q_{abs}\left(s, \epsilon_{eff}, \lambda\right) B_\odot(\lambda)\, d\lambda, \tag{3}$$

$$E_r = 4\pi \int_0^\infty A Q_{abs}\left(s, \epsilon_{eff}, \lambda\right) B(\lambda, T)\, d\lambda, \tag{4}$$

where $Q_{abs}(s, \epsilon_{eff}, \lambda)$ is the absorption efficiency of the aggregate evaluated by Mie theory. The solid angle subtended by the sun at a solar distance r is given by $\Omega = 2\pi\{1 - [1 - (R_\odot/r)^2]^{1/2}\}$. When $r >> R_\odot$, $\Omega \cong \pi\left(R_\odot/r\right)^2$. The solar flux $B_\odot(\lambda)$ at a wavelength of λ is compiled in Mukai (1990) for wavelength ranges of $\lambda = 0.14 - 300$ μm. Because of the limitation for the validity of the Bruggeman mixing rule, we set $s_0 = 0.01$ μm ($<< \lambda$) for the following calculations. The Planck function $B(\lambda, T)$ at the temperature T of the aggregate is defined by $B(\lambda, T) = 2hc^2\lambda^{-5}[\exp(hc/\lambda k_B T) - 1]^{-1}$, where h, k_B, and c are the Planck constant, the Boltzmann constant, and the speed of light, respectively.

The rate of sublimated energy E_s for the composite aggregate consisting of n-component materials with the total effective area S of sublimating surface is expressed as

$$E_s = S \sum_{i=1}^{n} \alpha_i \tilde{f}_i \sqrt{\frac{\mu_i m_u}{2\pi k_B T}}\, p_i(T)\, L_i, \tag{5}$$

where the subscript i denotes the i-th component of the dust aggregate; α_i means a reduction rate from the pure theoretical prediction and is called the accommodation coefficient; and m_u is the atomic mass unit. The mean molecular weight μ_i for vacuum is taken as zero. The saturated vapor pressure $p_i(T)$ of the i-th material at the dust temperature T is given by

$$p_i(T) = \exp\left(-\frac{\mu_i m_u}{k_B T} L_i + b_i\right). \tag{6}$$

The equilibrium temperature $T(s, r)$ of a fractal aggregate with its characteristic radius s at a solar distance r is determined by solving the balance equation of energy, $E_a = E_r + E_s$. Using the relation $S = 4A$ for the fractal dust (Kitada et al. 1993), the equation reduces to

$$\begin{aligned} &\Omega \int_0^\infty Q_{abs}\left(s, \epsilon_{eff}, \lambda\right) B_\odot(\lambda)\, d\lambda \\ &= 4\pi \int_0^\infty Q_{abs}\left(s, \epsilon_{eff}, \lambda\right) B(\lambda, T)\, d\lambda \\ &+ 4 \sum_{i=1}^{n} \alpha_i \tilde{f}_i \sqrt{\frac{\mu_i m_u}{2\pi k_B T}}\, p_i(T)\, L_i. \end{aligned} \tag{7}$$

In the one component case of homogeneous spherical dust, Eq. (7) becomes the already familiar expression (cf. Lamy 1974b).

Figs. 2 and 3 show the equilibrium temperatures T of the fractal aggregates consisting of silicate and carbon material, respectively, at a solar distance of 10 $R_\odot$ versus their characteristic radii $s = 0.05 - 50$ μm. In comparison with the equilibrium temperature of a homogeneous sphere without porosity, that of the fractal aggregate becomes independent of its radius. The temperature of the highly porous aggregate approaches the value of the constituent particles as demonstrated by Greenberg & Hage (1990). These results are independent of chemical composition, and agree with that in Kozasa et al. (1992) where the temperatures of magnetite aggregates were calculated under no sublimation.

The temperature of the fluffy aggregate consisting of silicate material becomes low and far from the blackbody temperature with $Q_{abs} = 1$. On the other hand, the temperature of the carbon aggregate, in spite of its absorbing property, differs from that of the blackbody except for the large ($s > 10$ μm) aggregate with small porosity. Consequently, the blackbody approximation fails to represent the temperature of irregularly shaped particles with fluffy structure, even for absorbing materials.

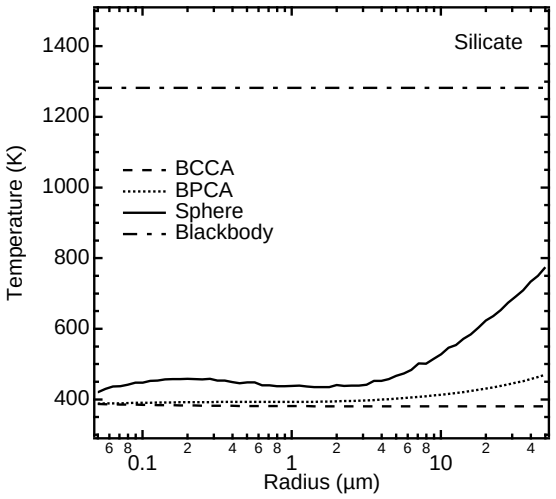

Fig. 2. Temperature of the fractal aggregate consisting of silicate constituent particles at a solar distance of 10 $R_\odot$ versus its characteristic radius.

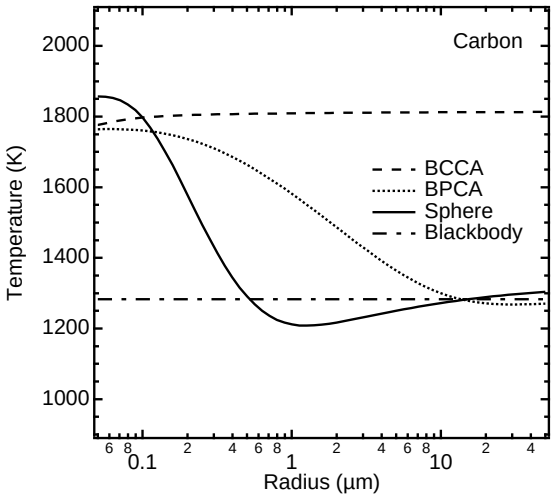

Fig. 3. The same as Fig. 2, but for carbon.

A lower temperature with the same chemical composition decreases the heliocentric distance of the sublimation zone. Accordingly, the sublimation zone of silicate aggregates approaches the sun, compared with that of silicate compact spheres. On the other hand, the carbon aggregates with high porosity begin sublimation far from the sun, compared with carbon compact spheres. It is worthwhile to notice that the accommodation coefficient α_i in Eq. (5) is assumed to be unity for simplicity. If we take a smaller value of the accommodation coefficient than unity, the equilibrium temperature obtained from Eq. (7) increases to compensate for the decrease of E_s. Consequently, the solar distance of the sublimation zone will increase by more than the value acquired from the above result.

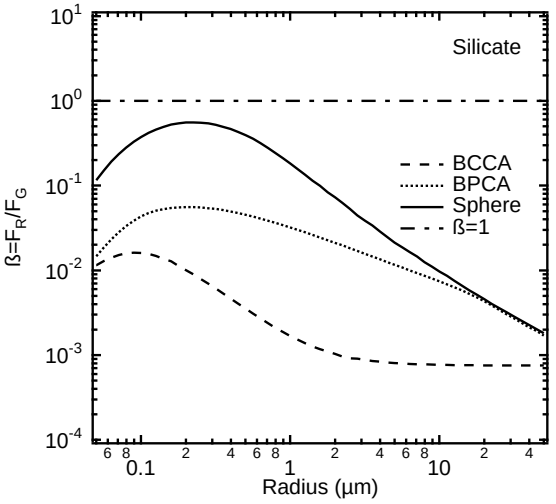

Fig. 4. The ratio β of the radiation pressure force to the solar gravity on the fractal aggregate consisting of silicate constituent particles versus its characteristic radius.

4. Radiation pressure force

The relative importance of the radiation pressure force F_R to the solar gravitational force F_G is described by a ratio $\beta = F_R/F_G$. The ratio β for a fractal aggregate is calculated as follows

$$\beta = \frac{r^2\Omega}{GM_\odot c}\left(\frac{A}{m}\right)\int_0^\infty B_\odot(\lambda)\, Q_{pr}\left(s, \epsilon_{eff}, \lambda\right) d\lambda, \qquad (8)$$

where $Q_{pr}(s, \epsilon_{eff}, \lambda)$ is the radiation pressure efficiency of the aggregate calculated using Mie theory. The gravitational constant and the mass of the sun are given by G and $M_\odot$, respectively. The mass m of the composite aggregate without taking into account sublimation is expressed as

$$m = \frac{4}{3}\pi {s_0}^3 \alpha \left(\frac{s}{s_0}\right)^D \sum_{i=1}^{n} \tilde{f}_i \rho_i, \qquad (9)$$

where the bulk density ρ_i for vacuum is set to zero. We make use of the data for the solar flux $B_\odot(\lambda)$, instead of the Planck function $B(\lambda, T = 5778\ \mathrm{K})$ used in Mukai et al. (1992). When the aggregate is composed of one-component material, Eq. (8) corresponds to that in Mukai et al. (1992). Furthermore, it is noted that in the near solar region the β ratio becomes a function of a solar distance due to a deviation of Ω from r^{-2} relation as well as an aggregate radius s.

The β ratio for the fractal aggregate as a function of its radius is plotted in Figs. 4 and 5 for $r >> R_\odot$. In contrast to a strong radius-dependence of the β ratio for a compact sphere, the β ratio for the fractal aggregate has a gentle slope as a function of its radius. Therefore, when the radius of the aggregate decreases due to sublimation, the β ratio for the fractal aggregate hardly changes. Since the value of β for a fractal aggregate consisting of silicate falls below unity, the silicate aggregates as well as the spherical particles stay in their sublimation zones. On the other hand, the carbon aggregate with low porosity escapes from

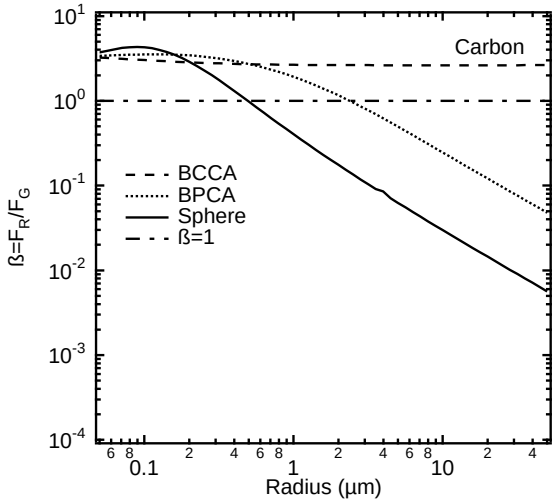

Fig. 5. The same as Fig. 4, but for carbon.

the vicinity of the sun before its characteristic radius reaches 2 μm due to sublimation, while spherical carbon grains for radii $s < 0.5$ μm are blown away from the solar system (Mukai & Mukai 1973). Furthermore, the value of β for the carbon aggregates with large porosity exceeds unity in all ranges of the radius. Consequently, it is difficult for the porous aggregates consisting of carbon material to survive in the solar system.

5. Dust-free zone

A ratio of dust lifetime due to sublimation $T_s \equiv s/\left|ds/dt\right|$ to its Keplerian period $T_K \equiv 2\pi\sqrt{r^3/GM_\odot(1-\beta)}$ is used to estimate the solar distance of the sublimation zone (Mukai & Yamamoto 1979). In order to obtain the value of T_s for the fractal aggregate, it is necessary to derive an expression of ds/dt. We assume a relation $dm/dt = D\left(m/s\right) ds/dt$ because $m \propto s^D$ (see Eq. (9)). The mass sublimation rate dm/dt of the aggregate is given by

$$\frac{dm}{dt} = -S\sum_{i=1}^{n}\tilde{f}_i\sqrt{\frac{\mu_i m_u}{2\pi k_B T}}p_i\left(T\right). \tag{10}$$

Accordingly, T_s/T_K for fluffy aggregate becomes

$$\frac{T_s}{T_K} = \sqrt{\frac{GM_\odot\left(1-\beta\right)}{4\pi^2 r^3}}D\frac{m}{\left|dm/dt\right|}. \tag{11}$$

When $S = 4\pi s^2$, this expression for T_s/T_K is consistent with that in Mukai & Yamamoto (1979).

The location of the closest approach to the sun for the dust grains suffering sublimation is called the edge of the dust-free zone, which is estimated from a heliocentric distance of $T_s/T_K = 10^2$ by Mukai & Yamamoto (1979). As shown in Fig. 6, the edge of the dust-free zone is sensitive to the carbon content. In the following calculations, we use the silicate aggregate containing carbon of 0.06 % in the volume because it sublimes at 4 $R_\odot$. This result coincides with that derived from Mann et al. (1994).

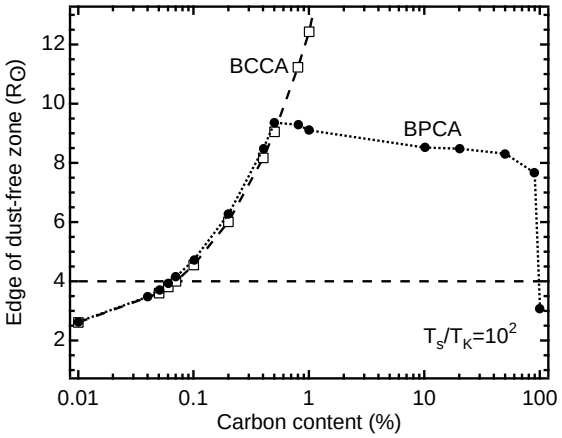

Fig. 6. Edge of the dust-free zone in the range of carbon content from 0.01 to 100 %. Filled circle: BPCA; open square: BCCA.

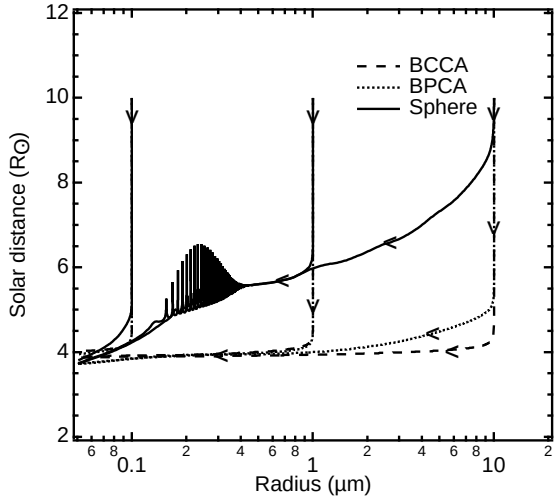

Fig. 7. Trajectories of the fractal aggregates in the $r - s$ plane. The initial condition is taken as e = 0 at a solar distance of 10 $R_\odot$.

6. Spatial number density

In the field of solar gravity and radiation, the equation of motion for the dust in terms of order v/c is expressed as (Robertson 1937)

$$\frac{d^2\mathbf{r}}{dt^2} = -\frac{GM_\odot}{r^2}\hat{\mathbf{S}} + \frac{GM_\odot}{r^2}\beta\left[\left(1-\frac{\mathbf{v}\cdot\hat{\mathbf{S}}}{c}\right)\hat{\mathbf{S}} - \frac{\mathbf{v}}{c}\right], \tag{12}$$

where $\hat{\mathbf{S}}$ is a unit vector of radial direction and $\mathbf{v}$ is a velocity vector of the aggregate. To calculate dynamical evolution of fluffy aggregate near the sun, we integrate Eqs. (10) and (12), simultaneously. Since the Poynting-Robertson effect reduces the eccentricity e and the semimajor axis a gradually (Wyatt & Whipple 1950), the eccentricity of the grain becomes sufficiently small near the sun. Therefore, the initial condition is taken as e = 0 at a solar distance of 10 $R_\odot$.

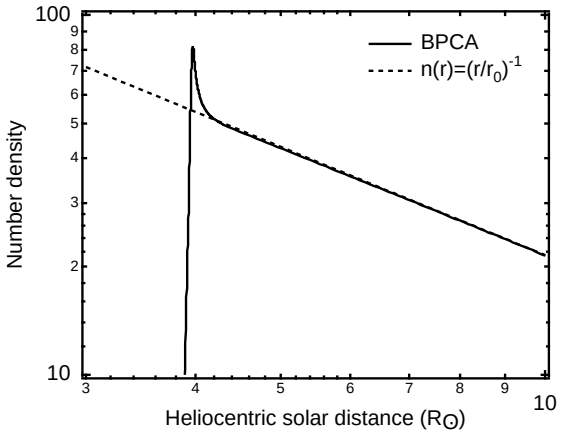

Fig. 8. Number density distribution of the BPCA normalized at r_0 = 1 AU.

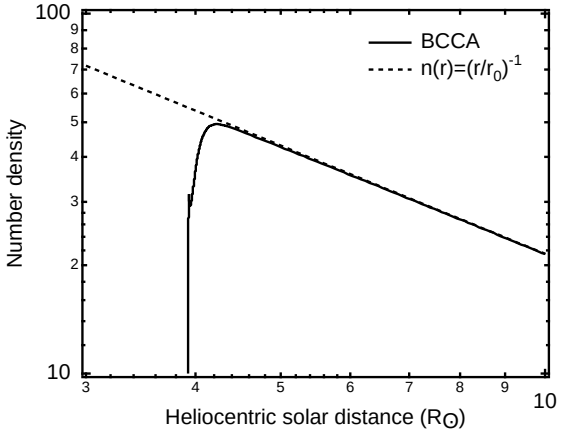

Fig. 9. The same as Fig. 8, but for the BCCA.

The trajectories of the fractal aggregates, including those of homogeneous spheres, in the $r - s$ plane are shown in Fig. 7. The fractal aggregates with different radii sublimate at the same solar distance of 4 $R_\odot$ in contrast to a strong size-dependence of the sublimation zone for homogeneous spheres. Although the orbit of a homogeneous sphere becomes elliptic for particles of sub-micron size, a fractal aggregate keeps a circular orbit (e = 0) as a consequence of the rather weak dependence of the β ratio on its radius. It is proved from Fig. 7 that T_s/T_K in Eq. (11) gives the location of the sublimation zone for fluffy dust aggregate.

When the inward dust flux is in equilibrium, the spatial number density $n(r)$ of the aggregate at a solar distance r is derived from the relation, $n(r)r^2dr/dt$ =const., where dr/dt denotes the radial component of the speed of the aggregate. Under the Poynting-Robertson effect without sublimation, $n(r) \propto r^{-1}$ because $dr/dt \propto r^{-1}$ in a circular orbit. Figs. 8 and 9 show the number density distributions of the fractal aggregates normalized at r_0 = 1 AU against the heliocentric distance. The fractal aggregates with different sizes accumulate at the same distance from the sun because of the independence of the sublimation zone on their radii (Fig. 8). Consequently, the spatial number density of the BPCA increases in a narrower region than that of the spherical particles. The spatial concentration of the BPCA in the sublimation zone becomes a factor of 1.5 relative to the spatial number density expected by its radial velocity due to the Poynting-Robertson effect alone. This concentration factor of the spatial distribution for the silicate-carbon BPCA is less than the factor of 5 for spherical silicate expected by Mukai & Yamamoto (1979). In the case of the BCCA, an enhancement of the spatial number density does not occur near the sublimation zone (Fig. 9).

7. Discussion

We will discuss the faint dust ring of the BPCA silicate and the edge of the dust-free zone of the BCCA silicate from the observational point of view. Expected brightness of the solar corona B_{K+F} at a wavelength range λ to $\lambda + d\lambda$ is calculated as

$$B_{K+F} = B_{th} + B_{sca} + B_K, \quad (13)$$

$$B_{th} = \int_0^\infty dl \int_{s_1}^{s_2} dsf(s,r)\, AQ_{abs}(s,\lambda)\, B(\lambda,T), \quad (14)$$

$$B_{sca} = \int_0^\infty dl \int_{s_1}^{s_2} dsf(s,r)\, \frac{i_1+i_2}{2k^2}\Omega B_\odot(\lambda), \quad (15)$$

$$B_K = \int_0^\infty dl N_e(r)\, \sigma_T \Omega B_\odot(\lambda), \quad (16)$$

where B_{th}, B_{sca}, and B_K denote the brightness of thermal emission from dust particles, their scattered sunlight along the line of sight, and the K-corona, respectively. We use a model from Saito et al. (1977) for the electron density $N_e(r)$ at a solar distance r; σ_T is the electron cross section of the classical Thomson scattering; l is a distance of the dust from an observer along the line of sight; $k = 2\pi/\lambda$ is the wave number of λ; and $f(s,r)$ is the radius and spatial distribution of dust grains, where $f(s,r)$ is assumed as a product of the number density distribution $n(r)$ and the size distribution $g(s)$. The results shown in Figs. 8 and 9 are used for a determination of $n(r)$. We derive $g(s)$ from the interplanetary flux model given by Grün et al. (1985) and then set the total cross-sectional area as $\int_{s_1}^{s_2} dsAg(s) = 4.6 \times 10^{-19}$ m^2/m^3. The Mie intensity functions perpendicular and parallel to the scattering plane are given by i_1 and i_2, respectively. We set s_1 = 0.01 μm and s_2 = 1000 μm.

Fig. 10 shows the expected visible (λ = 0.55 μm) brightness of the solar corona from the silicate-carbon BPCA, and the observations by Blackwell et al. (1967) and Saito et al. (1977). As a result of the faint solar dust ring, the enhancement of scattered light expected by the solar dust ring model for spherical particles disappears in the visible brightness of the solar corona. The expected visible brightness decreases smoothly with increasing radial distance R, and this expected feature, including its absolute values, agrees with visible observations. Even in the near-infrared (λ = 2.2 μm), it is hard to observe such a silicate dust ring (Fig. 11), because of the low temperature and therefore weak thermal emission at 4 $R_\odot$, compared to the blackbody. Since the temperature of BCCA silicate is lower than that of BPCA and thus farther from the blackbody temperature, the

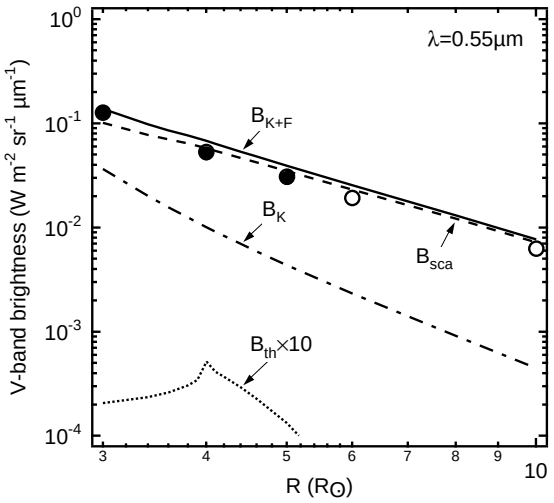

Fig. 10. Calculated V-band (λ = 0.55 μm) brightness of the solar corona B_{K+F} with the interplanetary flux model from Grün et al. (1985). Dash-dotted line: K-corona B_K; dotted line: thermal emission B_{th}; dashed line: scattered light B_{sca}; solid line: expected brightness $B_{K+F} = B_K + B_{th} + B_{sca}$. Open circle: Blackwell et al. (1967); filled circle: Saito et al. (1977).

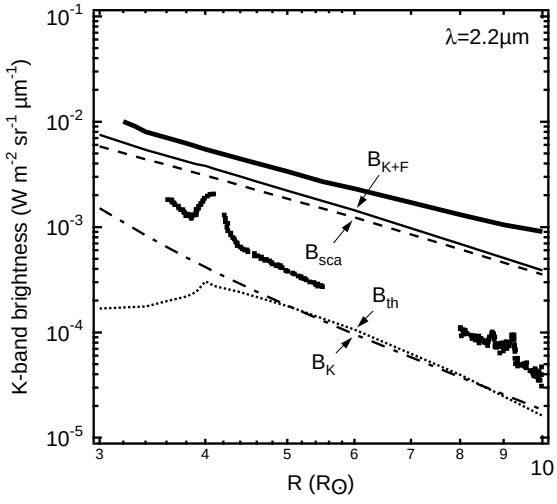

Fig. 11. Calculated K-band (λ = 2.2 μm) brightness of the solar corona B_{K+F} with the interplanetary flux model from Grün et al. (1985). Dash-dotted line: K-corona B_K; dotted line: thermal emission B_{th}; dashed line: scattered light B_{sca}; solid line: expected brightness $B_{K+F} = B_K + B_{th} + B_{sca}$. Thick solid line: Hodapp et al. (1992); dots: MacQueen (1968).

edge of the dust-free zone from BCCA silicate is invisible in the near-infrared brightness.

Furthermore, the number density distribution $n(r)$ of dust used in this paper causes the disappearance of a hump in the brightness. In comparison with a power ν = 1.3 for $n(r) = (r/r_0)^{-\nu}$ at a farther distance from the sublimation zone used in Mukai & Yamamoto (1979), an exponent ν = 1 used in this paper diminishes the contribution of the near-solar dust to the total brightness. Consequently, the exponent ν = 1 brings about no feature of the solar dust ring and edge of the dust-free zone in the visible and near-infrared brightness. It is noteworthy that the power ν = 1 is not only supported theoretically by dynamical behaviour of dust under the Poynting-Robertson effect, but also by the analysis of the zodiacal light observations (Lamy & Perrin 1986). The power ν = 1.3 is also supported by the zodiacal light observations (Leinert et al. 1978). As shown in Fig. 10, the model visible brightness of the F-corona fulfills a relation of $B_{sca} \propto R^{-2.25}$ for $R > 4\ R_\odot$ derived by the zodiacal light observations (Koutchmy & Lamy 1985). In addition, the absolute magnitude of the model brightness corresponds to that of the observations from Blackwell et al. (1967) and Saito et al. (1977). Accordingly, an application of ν = 1.3 will result in a steeper brightness distribution of R than the zodiacal light observations and brighter solar corona than the observed coronal brightness.

Although an adoption of silicate including a large fraction of carbon causes higher thermal emission, they sublimate at a greater solar distance than at 4 $R_\odot$, where the thermal emission hump has been observed. The larger solar distance of highly contaminated silicate may correspond to the other near-infrared hump at near 9 $R_\odot$ (MacQueen 1968). On the other hand, it is seen from Fig. 6 that carbon aggregates with small impurities sublimate at 4 $R_\odot$ and, furthermore, from Fig. 5 that large ($s \geq 10$ μm) carbon aggregates with small porosity stay in the F-corona because of $\beta < 1$. As a result of their high temperatures, which lie near the blackbody temperature ($T \sim 2100$ K), large carbon aggregates will contribute to the near-infrared brightness in the F-corona. Moreover, the color temperature of 2160±200 K was derived from the near-infrared hump at 4 $R_\odot$ measured during the 1970 solar eclipse (Peterson 1971). Accordingly, the appearance of a thermal emission hump at 4 $R_\odot$ may indicate the existence of irregularly shaped particles consisting of carbon material in the F-corona as opposed to silicate: We conclude, therefore, that the near-infrared hump observed in the F-corona arises from thermal emission of absorbing material, like a blackbody used in Mann (1992).

In order to observe the faint dust ring or the edge of the dust-free zone of fluffy silicate dust, the intermediate infrared is suitable because of their high emissivity near 10 μm (Fig. 12). As shown in Fig. 6, however, the distance dependence of the sublimation zone on the impurities seems to smear the feature of the faint dust ring or the edge of the dust-free zone if silicate aggregates having different amounts of impurities exist in the F-corona at the same time. Although the absolute magnitude of the model brightness is one order smaller than Mankin et al. (1974) and two orders smaller than Léna et al. (1974), their higher brightnesses are questionable because of the high noise level. More low-noise observations in the intermediate infrared might clarify the existence of fluffy silicate dust in the F-corona.

8. Conclusion

Taking into account the shape and structure of circumsolar dust grains, we have examined their dynamical and radiative nature

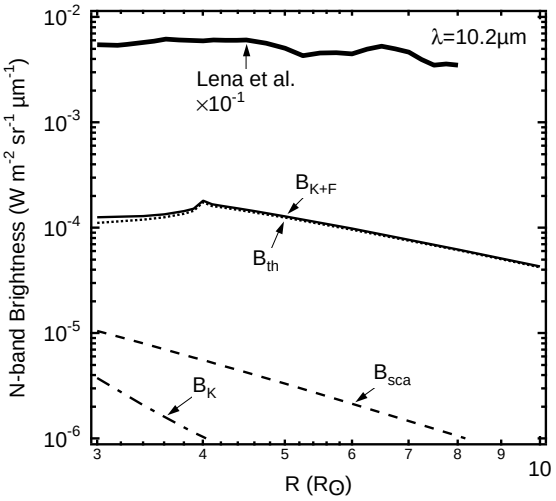

Fig. 12. Calculated N-band (λ = 10.2 μm) brightness of the solar corona B_{K+F} with the interplanetary flux model from Grün et al. (1985). Dash-dotted line: K-corona B_K; dotted line: thermal emission B_{th}; dashed line: scattered light B_{sca}; solid line: expected brightness B_{K+F} = B_K + B_{th} + B_{sca}. Thick solid line: Léna et al. (1974).

near the sun. Special attention has been placed on the differences from spherical homogeneous grains. We have found that the equilibrium temperature of a porous irregularly shaped particle, modeled here as a fractal aggregate, is independent of its size. As a result, fractal aggregates with different sizes begin their quick sublimation at the same solar distance. The location of sublimation for the fractal aggregate, therefore, is determined by the chemical composition alone. We have found that the peak feature in the F-corona indicates the existence of dust aggregate consisting of absorbing material rather than transparent material. If the irregularly shaped particles with porous structure make up the near-solar dust clouds, the solar dust ring indicates a small enhancement of number density with narrow spatial structure at the edge of sublimation zone or that it does not exist. This, however, does still not explain the fact of the "missing" dust ring during the 1991 eclipse.

Acknowledgements. H. Kimura would like to thank Dr. I. Mann for useful discussions and helpful suggestions while preparing this paper and Dr. P. Chilson for improving the English. The author also thanks Prof. J. M. Greenberg for his beneficial comments as a referee and Dr. N. V. Voshchinnikov, Dr. A. V. Krivov, P. Hillebrand, and A. Wehry for reviewing the original draft.

References

Belton M. J. S. 1966, Sci 151, 35
Blackwell D. E., Dewhirst D. W., Ingham M. F. 1967, Adv. Astron. Astrophys. 5, 1
Blum J., Kozasa T. 1992, in preparation
Brownlee D. E. 1976, In Elasässer H., Fechtig H. (eds.), Interplanetary Dust and Zodiacal Light, Vol. 48 of Lecture Notes in Physics IAU, Springer-Verlag, p.279
Centolanzi F. J., Chapman D. R. 1966, J. Geophys. Res. 71, 1735
Clarke J. T., Fox B. R. 1969, J. Chem. Phys. 51(8), 3231
Greenberg J. M., Hage J. I. 1990, ApJ 361, 260
Grün E., Zook H. A., Fechtig H., Giese R. H. 1985, Icarus 62, 244
Hanner, M. 1987, In Hanner M. (ed.), Infrared Observations of Comets Halley & Wilson and Properties of the Grains, NASA Conference, p.22
Hodapp K.-W., MacQueen R. M., Hall D. N. B. 1992, Nat 355(20), 707
Jones A. P. 1988, MNRAS 234, 209
Kitada Y., Nakamura R., Mukai T. 1993, In Maeda M. (ed.), The Third International Congress on Optical Particle Sizing, p.121
Koutchmy S., Lamy P. L. 1985, In Giese R. H., Lamy P. L. (eds.), Properties and Interactions of Interplanetary Dust, Astrophysics and Space Science Library, IAU, D. Reidel, p.63
Kozasa T., Blum J., Mukai T. 1992, A&A 263, 423
Lamy P. L. 1974a, A&A 33, 191
Lamy P. L. 1974b, A&A 35, 197
Lamy P. L., Perrin J.-M. 1986, A&A 163, 269
Leinert C., Hanner M., Pitz E. 1978, A&A 63, 183
Léna P., Viala Y., Hall D., Soufflot A. 1974, A&A 37, 81
Lide D. R. 1994, CRC Handbook of Chemistry and Physics, 75th edition, CRC, p.4-50
MacQueen R. M. 1968, ApJ 154, 1059
Mankin W. G., MacQueen R. M., Lee R. H. 1974, A&A 31, 17
Mann I. 1992, A&A 261, 329
Mann I., Okamoto H., Mukai T., Kimura H., Kitada Y. 1994, A&A 291, 1011
Mukai T. 1990, In Bonetti A., Greenberg J. M., Aiello S. (eds.), Evolution of Interstellar Dust and Related Topics, Elsevier Science, p.397
Mukai T., Ishimoto H., Kozasa T., Blum J., Greenberg J. M. 1992, A&A 262, 315
Mukai T., Mukai S. 1973, PASJ 25(4), 481
Mukai T., Yamamoto T. 1979, PASJ 31, 585
Mukai T., Yamamoto T., Hasegawa H., Fujiwara A., Koike, C. 1974, PASJ 26, 445
Peterson A. W. 1963, ApJ 138, 1218
Peterson A. W. 1967, ApJ 148, L37
Peterson A. W. 1969, ApJ 155, 1009
Peterson A. W. 1971, BAAS 3(4), 500
Robertson H. P. 1937, MNRAS 97(6), 423
Saito K., Poland A. I., Munro R. H. 1977, Solar Phys. 55, 121
Wyatt S. P. Whipple F. L. 1950, ApJ 111, 134

This article was processed by the author using Springer-Verlag LaTeX A&A style file *L-AA* version 3.